

Article

Thermodynamic Analysis of Low-Emission Offshore Gas-to-Wire Firing CO₂-Rich Natural Gas: Aspects of Carbon Capture and Separation Systems

Alessandra de Carvalho Reis, Ofélia de Queiroz Fernandes Araújo  and José Luiz de Medeiros * Escola de Química, Federal University of Rio de Janeiro, CT, E, Ilha do Fundão,
Rio de Janeiro 21941-909, RJ, Brazil; ofelia@eq.ufrj.br (O.d.Q.F.A.)

* Correspondence: jlm@eq.ufrj.br

Abstract: Despite the growth of renewable energy, fossil fuels dominate the global energy matrix. Due to expanding proved reserves and energy demand, an increase in natural gas power generation is predicted for future decades. Oil reserves from the Brazilian offshore Pre-Salt basin have a high gas-to-oil ratio of CO₂-rich associated gas. To deliver this gas to market, high-depth long-distance subsea pipelines are required, making Gas-to-Pipe costly. Since it is easier to transport electricity through long subsea distances, Gas-to-Wire instead of Gas-to-Pipe is a more convenient alternative. Aiming at making offshore Gas-to-Wire thermodynamically efficient without impacting CO₂ emissions, this work explores a new concept of an environmentally friendly and thermodynamically efficient Gas-to-Wire process firing CO₂-rich natural gas (CO₂ > 40%mol) from high-depth offshore oil and gas fields. The proposed process prescribes a natural gas combined cycle, exhaust gas recycling (lowering flue gas flowrate and increasing flue gas CO₂ content), CO₂ post-combustion capture with aqueous monoethanolamine, and CO₂ dehydration with triethylene glycol for enhanced oil recovery. The two main separation processes (post-combustion carbon capture and CO₂ dehydration) have peculiarities that were addressed at the light shed by thermodynamic analysis. The overall process provides 534.4 MW of low-emission net power. Second law analysis shows that the thermodynamic efficiency of Gas-to-Wire with carbon capture attains 33.35%. Lost-Work analysis reveals that the natural gas combined cycle sub-system is the main power destruction sink (80.7% Lost-Work), followed by the post-combustion capture sub-system (14% Lost-Work). These units are identified as the ones that deserve to be upgraded to rapidly raise the thermodynamic efficiency of the low-emission Gas-to-Wire process.

Keywords: gas-to-wire; exhaust gas recycle; post-combustion carbon capture; CO₂ dehydration; monoethanolamine; triethylene glycol; thermodynamic analysis



Citation: Reis, A.d.C.; Araújo, O.d.Q.F.; de Medeiros, J.L. Thermodynamic Analysis of Low-Emission Offshore Gas-to-Wire Firing CO₂-Rich Natural Gas: Aspects of Carbon Capture and Separation Systems. *Gases* **2024**, *4*, 41–58. <https://doi.org/10.3390/gases4020003>

Academic Editor: Ben J. Anthony

Received: 12 December 2023

Revised: 27 February 2024

Accepted: 19 March 2024

Published: 25 March 2024



Copyright: © 2024 by the authors. Licensee MDPI, Basel, Switzerland. This article is an open access article distributed under the terms and conditions of the Creative Commons Attribution (CC BY) license (<https://creativecommons.org/licenses/by/4.0/>).

1. Introduction

Global warming concerns have been the subject of several international agreements. The rising utilization of renewable energies is a remarkable fact; however, fossil fuels still lead the global energy matrix. A large increase in natural gas power generation is expected in the next decades as a result of the expanding natural gas (NG) reserves and considering that NG is the cleanest fossil fuel [1].

Deep-water oil reserves of the Brazilian Pre-Salt offshore layer have a high gas–oil ratio, with CO₂-rich associated gas (CO₂ > 40%mol) [2]. Despite the low-quality gas, large investments in long-distance subsea pipelines are necessary to carry this NG to market [3].

In this scenario, an alternative to bypass both CO₂ and NG transport infrastructures (Gas-to-Pipe) is to install floating Gas-to-Wire (GTW) plants, adopting NG Combined Cycle (NGCC) power plants [4]. These plants, placed on the offshore gas field, convert the raw produced gas directly into electricity, which is exported to onshore facilities through long-distance High-Voltage Direct Current (HVDC) cables [5] for less losses [6].

Existing offshore GTW plants (≈ 600 MW) are not concerned with the destination of CO_2 , sending it into the atmosphere. To mitigate CO_2 emissions, GTW must include carbon capture and storage (CCS) to achieve emission goals [7] by decreasing the carbon footprint of power generation [8]. Captured CO_2 reinjection into the reservoir as Enhanced Oil Recovery (EOR) fluid [9] is a solution for CO_2 storage while improving oil production [10], as well as offering additional monetary leverage [11]. Hassanpouryouzband et al. [12] showed that more than 90% of the injected stream of CO_2 can be stored. Hassanpouryouzband et al. [13] pointed out that it is essential to control the injection pressure to enhance CO_2 storage efficiency. Hydraulic fracturing increases the permeability of oil and gas reservoirs [14], improving CO_2 storage [15].

Araújo et al. [16] evaluated CCS technologies, such as chemical absorption, physical absorption, membrane permeation, and hybrids. These authors detected that chemical absorption holds the lowest CO_2 emission per ton of injected CO_2 . Hetland et al. [17] performed theoretical GTW-CCS research, studying the implementation of post-combustion carbon capture (PCC) downstream a Siemens-NGCC. In their system, the NGCC plant flue gas was sent to a PCC unit using aqueous monoethanolamine (MEA). The authors pointed out that the GTW-CCS concept is feasible, although CO_2 -EOR stream dehydration was not taken into account.

Aiming to achieve the carbon neutrality of GTW-CCS processes, the implementation of gas turbine exhaust gas recirculation (EGR) has been considered in the literature [18]. By lowering the exhaust gas flowrate and increasing its CO_2 content, EGR facilitates the CO_2 capture step, because a higher CO_2 content increases the driving force for CO_2 absorption, lowering column height, while a lower flue gas flowrate lowers column diameter. These both reduce the CCS penalty by lowering investment [19]. In addition, EGR diminishes NOX emissions, since the circulating oxygen and nitrogen concentrations decrease in the cycle [20].

To implement GTW-CCS over offshore deep-water oil and gas fields, the process must include the following: (i) EGR; (ii) post-combustion carbon capture from CO_2 -rich flue gas via absorption in aqueous monoethanolamine (aqueous-MEA), i.e., the PCC-MEA plant; (iii) CO_2 compression; (iv) high-pressure CO_2 dehydration (CO_2 -DEHY) for lower water content (≈ 200 ppm-mol), avoiding CO_2 hydrates [21]; and (v) dense CO_2 injection in the oil and gas field for EOR. Offshore GTW for CO_2 -rich NG with EGR, CCS, and CO_2 -DEHY is written here as GTW-EGR-CCS- CO_2 -DEHY.

There is a gap in the literature regarding the GTW-EGR-CCS- CO_2 -DEHY overall process, the singularities of its separation sub-systems—i.e., the PCC-MEA plant and CO_2 -DEHY plant—and the thermodynamic analysis of the overall system and its sub-systems (second law analysis). To fill this gap, the present work assesses GTW-EGR-CCS- CO_2 -DEHY and conducts a thermodynamic analysis of the overall system and sub-systems, as well as exploring the peculiarities of its separation sub-systems. Thermodynamic analysis identifies power destruction sinks and quantifies the Lost-Work of the overall system and its sub-systems, aiming to identify process units that should be improved to increase the overall thermodynamic efficiency.

2. Methods

Offshore GTW-EGR-CCS- CO_2 -DEHY, using CO_2 -rich NG and exporting CO_2 -to-EOR and power, was designed and simulated in Aspen-HYSYS 10 for technical and thermodynamic assessments. The necessary theory, process descriptions, process complexity, and methods are discussed in this section.

2.1. Process Framework

Figure 1 depicts a block diagram representing GTW-EGR-CCS- CO_2 -DEHY and sub-systems. Medium-capacity (≈ 600 MW) offshore GTW-EGR-CCS- CO_2 -DEHY structure comprehends the following: (i) NGCC plant; (ii) Direct-Contact Column (DCC) that cools down the flue gas; (iii) low-pressure PCC-MEA for CO_2 capture; (iv) first CO_2 Compression

Unit (CO₂-CMP-1); (v) high-pressure CO₂ dehydration unit (CO₂-DEHY) with triethylene-glycol (TEG) for water removal from the CO₂-to-EOR stream; (vi) CO₂ Stripping Gas Unit (STR-CO₂) that produces the stripping gas to the CO₂-DEHY reboiler; (vii) second CO₂ Compression Unit (CO₂-CMP-2) that sends CO₂-to-EOR; and (viii) EGR arrangement.

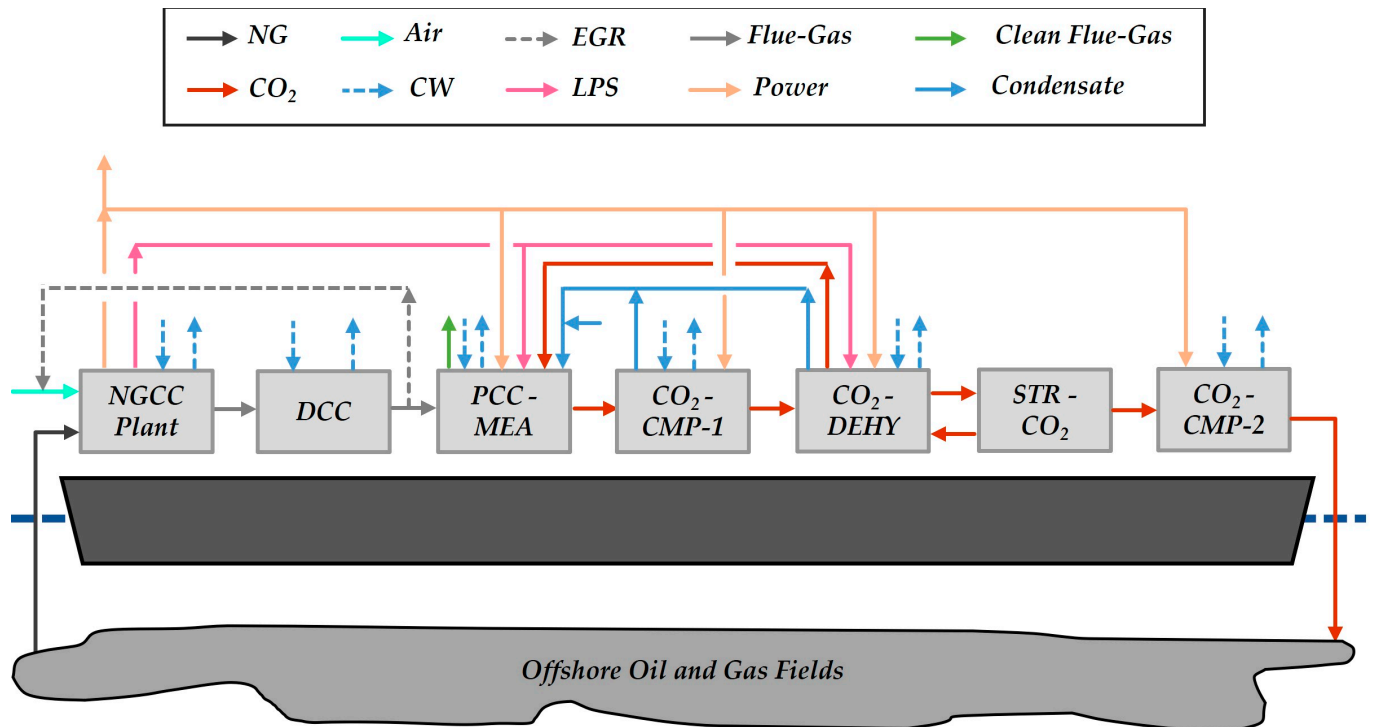


Figure 1. Process sub-systems (NGCC: NG Combined Cycle, DCC: Direct-Contact Column, PCC-MEA: post-combustion capture with aqueous-MEA, CO₂-CMP: CO₂ Compression Unit, CO₂-DEHY: CO₂ Dehydration TEG Unit, STR-CO₂: CO₂ Stripping Gas Unit, EGR: Exhaust Gas Recycle, CW: Cooling Water, LPS: Low-Pressure Steam).

2.1.1. Natural Gas Combined Cycle Plant

The NGCC plant comprises five NGCC elements for adequate electricity output (≈ 600 MW). As shown in Figure 2, each NGCC element contains four parallel gas turbines united to one Heat Recovery Steam Generator (HRSG), which heats a steam cycle (Rankine cycle). Aero-derivative gas turbines (Table 1) are applicable for offshore rigs considering their high power-to-weight ratio and low footprint [22]. Gas turbines fire raw CO₂-rich NG (CO₂ > 40%mol) without any conditioning. The generated flue gas feeds the HRSG at $T = 549$ °C [23], producing High-Pressure Superheated Steam (HPS) ($T = 524$ °C, $P = 24$ bar) and Low-Pressure Steam (LPS, $T = 160$ °C, $P = 6$ bar). Følgesvold et al. [24] presented the HRSG temperature approaches and head losses. The steam turbine receives the HPS and expands it to $P = 0.12$ bar. The resulting stream is cooled down in the sub-atmospheric condenser with Cooling Water (CW), arriving as condensation to the HRSG ($T = 45$ °C). The generated LPS heats PCC-MEA and CO₂-DEHY reboilers; therefore, the steam cycle power is controlled by LPS demand. The gas turbine model in HYSYS involves the following: (i) adiabatic single-stage air compressor; (ii) combustion chamber modeled as adiabatic conversion reactor; and (iii) adiabatic expander. This model was adjusted to manufacturing data by calibrating the adiabatic efficiencies of its air compressor and expander. Air is provided at stoichiometric proportion for complete NG combustion. To restrict the combustion temperature to factory settings, stoichiometric air is mixed with Exhaust Gas Recycle (EGR). Recycled flue gas is removed after the DCC and before the PCC-MEA, and its flowrate is adjusted to reach the prescribed flue gas temperature at the expander outlet ($T = 549$ °C).

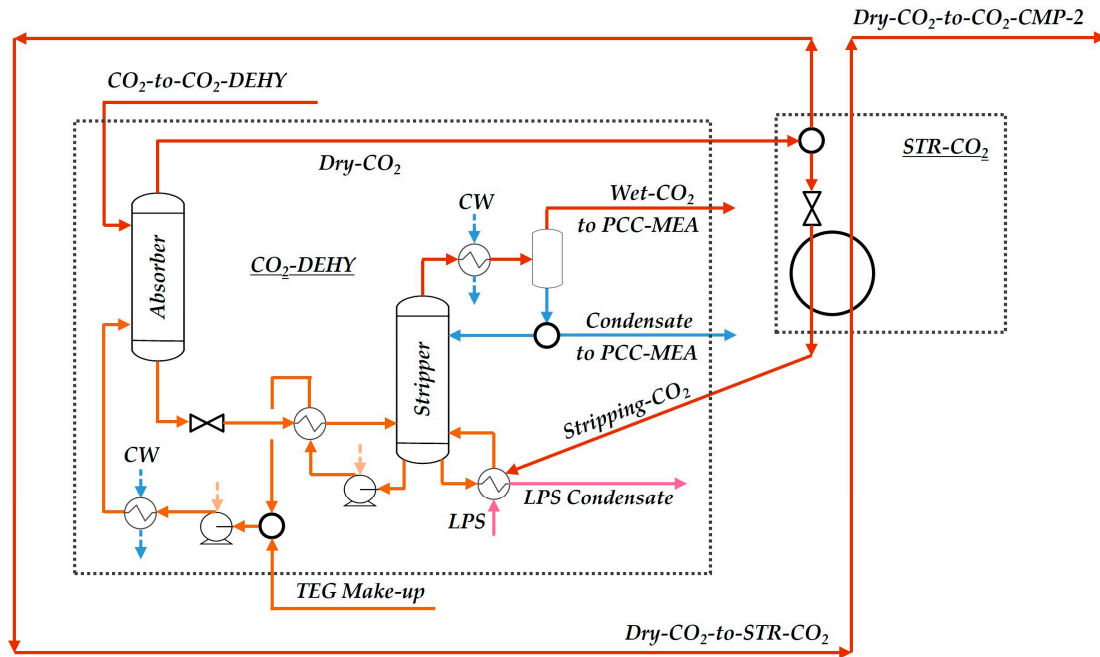


Figure 5. CO₂ Dehydration TEG Unit (CO₂-DEHY) and CO₂ Stripping Gas Unit (STR-CO₂) (PCC-MEA: Aqueous-MEA Post-Combustion Capture, CO₂-CMP: CO₂ Compression Unit, CW: Cooling Water, LPS: Low-Pressure Steam, HPS: High-Pressure Steam).

2.1.5. CO₂ Compression Units

CO₂-CMP-1 (Figure 6a) is a four-stage intercooled compression train (stage-compression ratio = 2.85) to increase the CO₂ stream pressure to 50 bar for feeding the CO₂-DEHY unit. CO₂-CMP-2 (Figure 6b) receives the Dry-CO₂ from STR-CO₂ and pressurizes the stream in order to reach the EOR pipeline pressure (P = 300 bar).

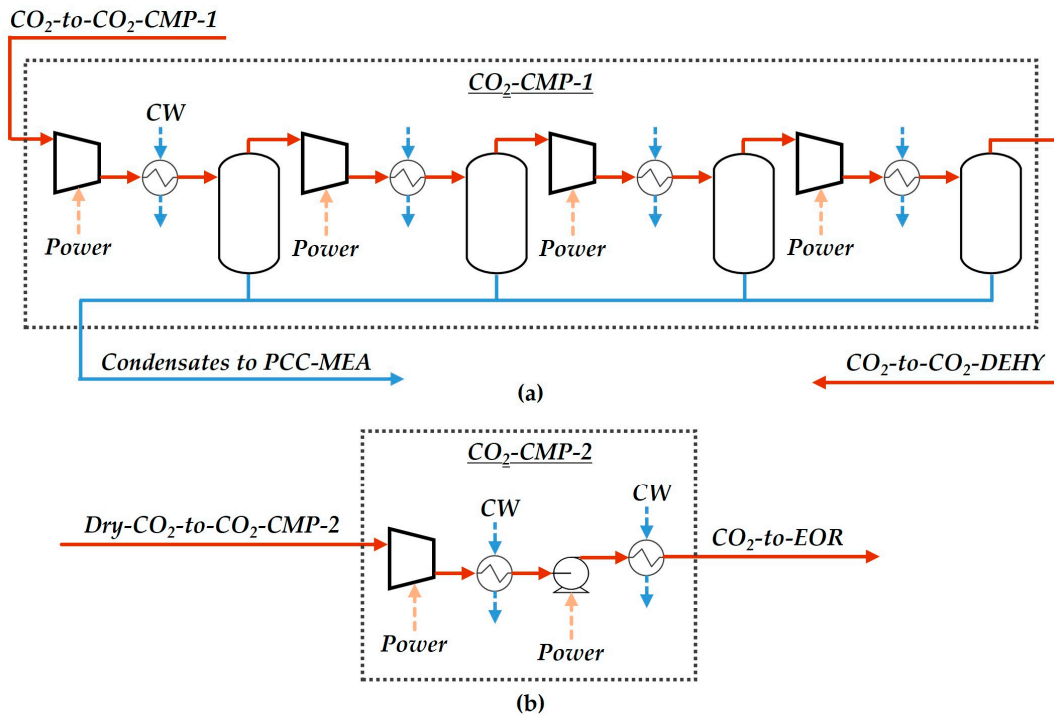


Figure 6. CO₂ Compression Units (CO₂-CMP): (a) CO₂-CMP-1 and (b) CO₂-CMP-2 (PCC-MEA: Aqueous-MEA Post-Combustion Capture, CO₂-DEHY: CO₂ Dehydration TEG Unit, EOR: Enhanced Oil Recovery, CW: Cooling Water).

2.1.6. Equipment Conditions and Process Simulation Assumptions

The main process simulation assumptions and equipment conditions are shown in Table 1.

Table 1. Simulation assumptions.

Item	Assumption
A1	Thermodynamic Models Gas streams: Peng–Robinson equation of state; Rankine cycle: ASME steam table; PCC-MEA: HYSYS Acid-Gas Package; CO ₂ -DEHY: HYSYS Glycol package.
A2	Air T = 25 °C; P = 1.013 bar; N ₂ = 77.14%mol; O ₂ = 20.51%mol; H ₂ O = 2.35%mol; [31].
A3	Raw CO ₂ -rich NG 6.5 MMSm ³ /d; T = 40 °C; P = 25 bar; CH ₄ = 49.82%mol, CO ₂ = 43.84%mol, C ₂ H ₆ = 2.99%mol, C ₃ H ₈ = 1.99%mol, iC ₄ H ₁₀ = 0.3%mol, C ₄ H ₁₀ = 0.2%mol, iC ₅ H ₁₂ = 0.2%mol, C ₅ H ₁₂ = 0.1%mol, C ₆ H ₁₄ = 0.1%mol, C ₇ H ₁₆ = 0.05%mol, C ₈ H ₁₈ = 0.03%mol, C ₉ H ₂₀ = 0.01%mol, C ₁₀ H ₂₂ = 0.01%mol, H ₂ O = 0.36%mol [2,31].
A4	Gas turbine Aero-Derivative GE LM2500 + G4; Efficiency ^{LHV} = 36.5%; P ^{Inlet} = 23 bar; [2,31] Air-Ratio = 6.2 mol/mol; T ^{Flue Gas} = 549 °C.
A5	Steam turbine HPS: P ^{Inlet} = 24 bar; P ^{Outlet} = 0.12 bar; T ^{Inlet} = 524 °C; Outlet-Quality = 98.1%; [31].
A6	Compressors Stage-compression ratio = 2.85; [2,31] Intercoolers: T ^{Gas-Outlet} = 35 °C; ΔT ^{Approach} = 5 °C; ΔP = 0.5 bar.H
A7	Adiabatic efficiencies η ^{Pumps} = η ^{Compressors} = η ^{Steam Turbine} = 75%; Gas Turbines: η ^{Air Compressor} = 87%, η ^{Expander} = 85.4%; [31].
A8	HRSG ΔP ^{Flue Gas} = 0.025 bar; ΔP ^{Steam} = 0.05 bar; ΔT ^{Approach} = 25 °C; [24].
A9	Exchangers ΔT ^{Approach} = 10 °C (gas-gas, liq-liq); ΔT ^{Approach} = 5 °C (gas-liq); ΔP = 0.5 bar; [31].
A10	DCC Stages ^{Theoretical} = 10; P ^{Top} = 1.053 bar; T ^{Top-Flue Gas} = 40 °C.
A11	PCC-MEA Absorber: Stages ^{Theoretical} = 40; P ^{Top} = 1.013 bar; T ^{Inlet-Top} = 40 °C; Capture = 90%; [31] Stripper: Stages ^{Theoretical} = 10; P ^{Top} = 1.013 bar; T ^{Top} = 40 °C; T ^{Reboiler} = 103 °C; [31] Lean-MEA: H ₂ O = 63.3%w/w, MEA = 31.6%w/w, CO ₂ = 5.1%w/w; [31] Capture Ratio: CR ≈ 14 kg ^{Solvent} /kg ^{CO₂} ; stripping Heat Ratio: HR ≈ 225 kJ/mol ^{CO₂} ; [31].
A12	CO ₂ -DEHY Absorber: Stages ^{Theoretical} = 15; P = 50 bar; T ^{Inlet} = 35 °C; Solvent: TEG = 98.5%w/w; Stripper: Stages ^{Theoretical} = 10; P ^{Top} = 1.013 bar; T ^{Top} = 40 °C; T ^{Reboiler} = 128 °C.
A13	CO ₂ -to-EOR T = 35 °C; P = 300 bar; Purity: CO ₂ ≥ 99.9%mol; [31].
A14	LPS P ^{LPS} = 6 bar, T ^{LPS} = 160 °C.
A15	Cooling Water CW: T ^{Inlet} = 30 °C; T ^{Outlet} = 45 °C; P ^{Inlet} = 4 bar; P ^{Outlet} = 3.5 bar.
A16	Steam production Priority: LPS ^{PCC-MEA} + LPS ^{CO₂-DEHY} ; Surplus: HPS ^{Rankine-Cycle} .

2.1.7. Complexity and Limitations of the New Offshore GTW-EGR-CCS-CO₂-DEHY Process

Ordinary NGCC plants at around 500 MW of capacity are feasible and quite simple plants that are already implemented in the offshore scenario of oil and gas production. However, existing ordinary NGCC plants are not concerned with the destination of CO₂, emitting it freely into the atmosphere. To mitigate CO₂ emissions, one solution is used in its reinjection into reservoirs via EOR. To make this possible, it is necessary to add the PCC-MEA (post-combustion CO₂ capture with aqueous-MEA) and the CO₂-DEHY (CO₂ dehydration) plants. Moreover, to lower the CCS costs, it is necessary to implement the Exhaust Gas Recycle (EGR), which reduces the flue gas flowrate (about 50% or higher reduction) and increases the flue gas content of CO₂ (about 100% or higher increase). The EGR is practically mandatory if CCS is involved because it raises the driving force for CO₂ absorption and reduces the volume of flue gas to be treated, consequently allowing for a reduction in column height and diameter and the number of absorbing columns. This way, the insertion of PCC-MEA, CO₂-DEHY, and EGR loop implies that there is a high increase in the number of recycling processes—the EGR itself and several recycles

of carbonated waters and CO₂ vapors to the stripper of PCC-MEA—which intrinsically increases the complexity of the process and negatively impacts its controllability. Thus, while a typically ordinary NGCC is a process with a simple direct structure, the proposed offshore GTW-EGR-CCS-CO₂-DEHY process is a reasonably complex one with a handicapped controllability—besides being a much more expensive process—which demands careful analysis of its global controllability and the possible interactions of different control actions during the design of its control and start-up systems. The problematic controllability configures the main shortcoming and limitation of the new proposed process because it may turn the process into a dynamically unstable system whose operation may entail risks and unexpected extra costs.

2.2. Thermodynamic Analysis of Steady-State Processes

Thermodynamic analysis is efficient to pinpoint resource degradation through processes. Steady-state offshore GTW-EGR-CCS-CO₂-DEHY and its sub-systems are evaluated by the second law analysis of processes. For the second law analysis, systems and their sub-systems are formerly classified as power-producing or power-consuming systems. Figure 7 exhibits a steady-state open system for thermodynamic assessment with numerous feed/product streams (blue/red arrows, respectively) interacting with an infinite isothermal heat reservoir (R_0) at temperature T_0 . The overall system and its sub-systems may be power-producing ($\dot{W} > 0$) or power-consuming ($\dot{W} < 0$), but they must only have thermal interactions with R_0 either absorbing ($\dot{Q} > 0$) or rejecting ($\dot{Q} < 0$) heat. $G_n, \bar{H}_{G_n}, \bar{S}_{G_n}$ represent, respectively, the molar flowrate (kmol/s), enthalpy (MJ/kmol), and entropy (MJ/kmol.K) of the n^{th} feed stream ($n = 1 \dots N_f$), while $K_n, \bar{H}_{K_n}, \bar{S}_{K_n}$ are similar for the n^{th} product stream ($n = 1 \dots N_p$).

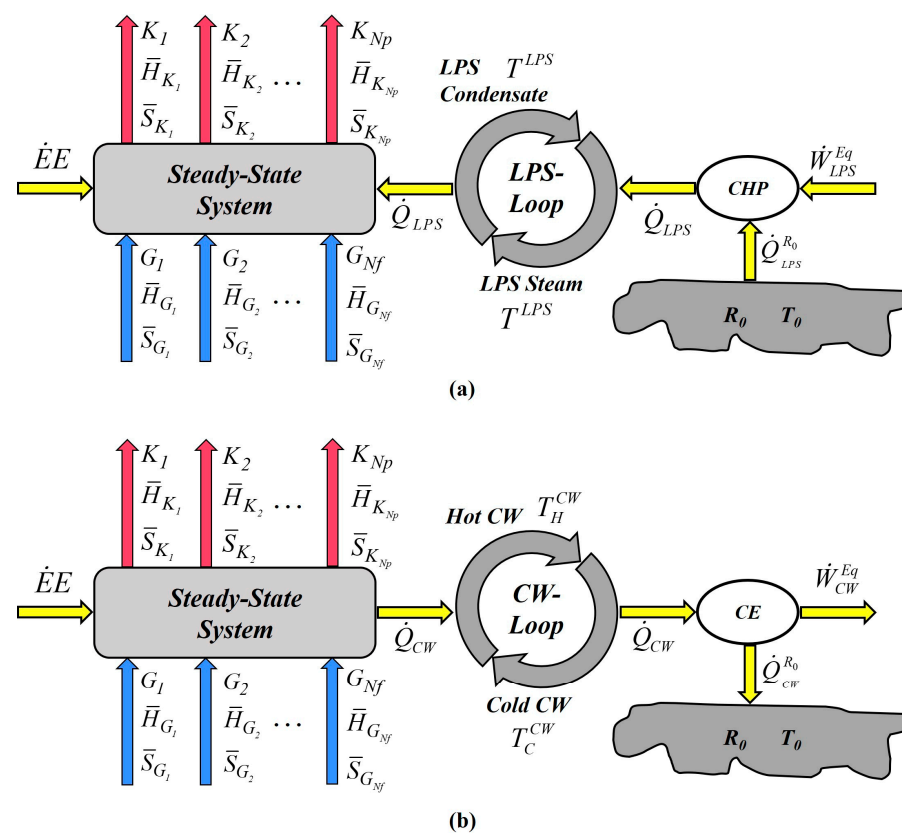


Figure 7. Equivalent power for power-consuming system (blue arrows: feed streams; red arrows: product streams): imports electricity ($\dot{E}E$); (a) imports equivalent power via LPS-Loop (\dot{W}_{LPS}^{Eq}); and (b) exports equivalent power via CW-Loop (\dot{W}_{CW}^{Eq}) (LPS: Low-Pressure Steam, CW: Cooling Water, CHP: Carnot Heat Pump, CE: Carnot Engine).

2.2.1. Maximum Power

Equations (1) and (2) depict the first law of thermodynamics applied to a steady-state open system (Figure 7). The system maximum power/work (\dot{W}^{MAX}) is calculated through the second law at reversible conditions adopting Equations (3)–(6). At reversible conditions, Equation (4) performs the universe entropy balance, making $\dot{S}^{UNIVREV}$ the universe entropy-creation rate. Under reversibility, Equation (5) derives from Equations (2) and (6), which result from Equation (4). Therefore, \dot{W}^{MAX} is given by Equation (7) or Equation (8). Equation (8) provides positive \dot{W}^{MAX} for power-producing systems (e.g., NGCC plant, DCC, and STR-CO₂) and negative \dot{W}^{MAX} for power-consuming Systems (e.g., PCC-MEA, CO₂-DEHY, CO₂-CMP-1, and CO₂-CMP-2).

$$\sum_{i=1}^{Np} G_i \bar{H}_{G_i} + \dot{Q} - \dot{W} = \sum_{i=1}^{Np} K_i \bar{H}_{K_i} \quad (1)$$

$$\dot{W} = - \left(\sum_{i=1}^{Np} K_i \bar{H}_{K_i} - \sum_{i=1}^{Nf} G_i \bar{H}_{G_i} \right) + \dot{Q} \quad (2)$$

$$\dot{W} = \dot{W}^{MAX}, \quad \dot{Q} = \dot{Q}^{REV} \quad (3)$$

$$\sum_{i=1}^{Np} K_i \bar{S}_{K_i} - \sum_{i=1}^{Nf} G_i \bar{S}_{G_i} - \frac{\dot{Q}^{REV}}{T_0} = \dot{S}^{UNIVREV} = 0 \quad (4)$$

$$\dot{W}^{MAX} = - \left(\sum_{i=1}^{Np} K_i \bar{H}_{K_i} - \sum_{i=1}^{Nf} G_i \bar{H}_{G_i} \right) + \dot{Q}^{REV} \quad (5)$$

$$\dot{Q}^{REV} = T_0 \left(\sum_{i=1}^{Np} K_i \bar{S}_{K_i} - \sum_{i=1}^{Nf} G_i \bar{S}_{G_i} \right) \quad (6)$$

$$\dot{W}^{MAX} = - \left(\sum_{i=1}^{Np} K_i \bar{H}_{K_i} - \sum_{i=1}^{Nf} G_i \bar{H}_{G_i} \right) + T_0 \left(\sum_{i=1}^{Np} K_i \bar{S}_{K_i} - \sum_{i=1}^{Nf} G_i \bar{S}_{G_i} \right) \quad (7)$$

$$\dot{W}^{MAX} = - \left(\sum_{i=1}^{Np} K_i (\bar{H}_{K_i} - T_0 \bar{S}_{K_i}) - \sum_{i=1}^{Nf} G_i (\bar{H}_{G_i} - T_0 \bar{S}_{G_i}) \right) \quad (8)$$

2.2.2. Equivalent Power

Being always positive for regular systems, \dot{W}^{Eq} represents the thermodynamic power equivalence of electricity production (consumption) and utility production (consumption) [31]. For example, LPS production (consumption) is equivalent to \dot{W}^{Eq} production (consumption), while CW consumption is always equivalent to \dot{W}^{Eq} production. Off-shore GTW-EGR-CCS-CO₂-DEHY demands three kinds of utilities: (i) electricity $\dot{E}E$ (MW); (ii) LPS with flowrate J^{LPS} (kmol/s), vaporization enthalpy $\Delta \bar{H}_{LPS}^{VAP}$ (MJ/kmol), and temperature T^{LPS} (K); and (iii) CW with flowrate J^{CW} (kmol/s), isobaric heat capacity \bar{C}_P^{CW} (MJ/kmol.K), and hot/cold temperatures T_H^{CW} (K), T_C^{CW} (K). Considering the LPS and CW narrow temperature ranges studied, $\Delta \bar{H}_{LPS}^{VAP}$ and \bar{C}_P^{CW} are assumed constants.

Heat power equivalences are calculated through reversible heat engines with the maximum heat work conversion yield, namely, the Carnot Heat Pump (CHP) and the Carnot Engine (CE) [31]. The CHP imports power, absorbs heat from a cold source, and rejects heat to a hotter source, while the CE absorbs heat from a hot source, exports power, and rejects heat to a colder one.

Figure 7 displays a power-consuming system with the following utility effects: absorbs $\dot{E}E$, absorbs heat \dot{Q}_{LPS} from LPS-Loop (imports power \dot{W}_{LPS}^{Eq}), and rejects heat \dot{Q}_{CW} to CW-Loop (exports power \dot{W}_{CW}^{Eq}). Figure 7 shows that the LPS-Loop and CW-Loop are external to the system (Figure 7), R_0 is always a cold heat reservoir (cold source), and \dot{W}_{LPS}^{Eq} , \dot{Q}_{LPS} , \dot{W}_{CW}^{Eq} , \dot{Q}_{CW} are always positive. It is possible to frame an analogous version of Figure 7 for a power-producing system (i.e., electricity and LPS are exported, and CW is imported).

The steady-state power-consuming system (Figure 7a) absorbs heat (\dot{Q}_{LPS}) from LPS, making it LPS-condensate, which is restored to LPS via a LPS-Loop, using the CHP, that imports power (\dot{W}_{LPS}^{Eq}) and absorbs heat ($\dot{Q}_{LPS}^{R_0}$) from R_0 . Similarly, the power-consuming system (Figure 7b) rejects heat (\dot{Q}_{CW}) to cold-CW, producing hot-CW, which is restored to cold-CW via a CW-Loop using the CE that exports power (\dot{W}_{CW}^{Eq}) and rejects heat ($\dot{Q}_{R_0}^{CW}$) to R_0 .

\dot{W}_{LPS}^{Eq} is given by Equation (10) using Equation (9a,b), and the CHP entropy conservation in Equation (9c). Accordingly, \dot{W}_{CW}^{Eq} is given by Equation (12) using Equation (11a,b), and the CE entropy conservation in Equation (11c). Equation (10) also works for \dot{W}_{LPS}^{Eq} in power-producing systems, but the LPS-Loop rotates counter-clockwise, the CHP is replaced by the CE, and all the effects are reversed.

Equation (13a) provides the equivalent power (\dot{W}^{Eq}) produced by a power-producing system that exports $\dot{E}E$ and LPS (counter-clockwise LPS-Loop in Figure 7) and consumes CW. Analogously, Equation (13b) gives the equivalent power consumed by a power-consuming system that consumes $\dot{E}E$, CW, and LPS. The substitution of Equations (10) and (12) into Equation (13a,b) results in Equation (14a,b) that give, respectively, the equivalent power produced by a power-producing system and the equivalent power consumed by a power-consuming system.

$$\dot{W}_{LPS}^{Eq} = \dot{Q}_{LPS} - \dot{Q}_{LPS}^{R_0} \quad (9a)$$

$$\dot{Q}_{LPS} = J^{LPS} \Delta \bar{H}_{LPS}^{VAP} \quad (9b)$$

$$-\frac{\dot{Q}_{LPS}^{R_0}}{T_0} + J^{LPS} \frac{\Delta \bar{H}_{LPS}^{VAP}}{T_{LPS}} = 0 \quad (9c)$$

$$\dot{W}_{LPS}^{Eq} = J^{LPS} \Delta \bar{H}_{LPS}^{VAP} \left(1 - \frac{T_0}{T_{LPS}} \right) \quad (10)$$

$$\dot{W}_{CW}^{Eq} = \dot{Q}_{CW} - \dot{Q}_{CW}^{R_0} \quad (11a)$$

$$\dot{Q}_{CW} = J^{CW} \bar{C}_P^{CW} (T_H^{CW} - T_C^{CW}) \quad (11b)$$

$$\frac{\dot{Q}_{CW}^{R_0}}{T_0} + J^{CW} \bar{C}_P^{CW} \ln \left(\frac{T_C^{CW}}{T_H^{CW}} \right) = 0 \quad (11c)$$

$$\dot{W}_{CW}^{Eq} = J^{CW} \bar{C}_P^{CW} \left(T_H^{CW} - T_C^{CW} - T_0 \cdot \ln \left(\frac{T_H^{CW}}{T_C^{CW}} \right) \right) \quad (12)$$

$$\dot{W}^{Eq} = \dot{E}E + \dot{W}_{LPS}^{Eq} + \dot{W}_{CW}^{Eq} \quad \{ \text{Power - Producing System} \} \quad (13a)$$

$$\dot{W}^{Eq} = \dot{E}E + \dot{W}_{LPS}^{Eq} - \dot{W}_{CW}^{Eq} \quad \{ \text{Power - Consuming System} \} \quad (13b)$$

$$\dot{W}^{Eq} = \dot{E}E + J^{LPS} \Delta \bar{H}_{LPS}^{VAP} \left(1 - \frac{T_0}{T_{LPS}} \right) + J^{CW} \bar{C}_P^{CW} \left(T_H^{CW} - T_C^{CW} - T_0 \cdot \ln \left(\frac{T_H^{CW}}{T_C^{CW}} \right) \right) \quad (14a)$$

$$\dot{W}^{Eq} = \dot{E}E + J^{LPS} \Delta \bar{H}_{LPS}^{VAP} \left(1 - \frac{T_0}{T_{LPS}} \right) - J^{CW} \bar{C}_p^{CW} \left(T_H^{CW} - T_C^{CW} - T_0 \cdot \ln \left(\frac{T_H^{CW}}{T_C^{CW}} \right) \right) \quad (14b)$$

2.2.3. Thermodynamic Efficiency

Process resource degradation is calculated via second law analysis, obtaining the thermodynamic efficiency and the Lost-Work (Lost-Power) of the overall system and its sub-systems. With \dot{W}^{MAX} (Equation (8)) and \dot{W}^{Eq} (Equation (14a,b)), the thermodynamic efficiencies of power-producing systems and power-consuming systems are given by Equation (15a) and Equation (15b), respectively.

$$\eta\% = 100 \cdot \dot{W}^{Eq} / \dot{W}^{MAX} \quad \{Power - Producing System\} \quad (15a)$$

$$\eta\% = 100 \cdot (-\dot{W}^{MAX}) / \dot{W}^{Eq} \quad \{Power - Consuming System\} \quad (15b)$$

2.2.4. Lost-Work

The Lost-Work (Lost-Power) formulas for power-producing systems and power-consuming systems are intuitively calculated by Equation (16a,b). Additionally, Lost-Work can be measured through the second law formula (Equation (17a)) that considers all the universe changes caused by system transitions, where \dot{S}^{UNIV} is the entropy-creation rate of the universe due to the system operation. Thus, Equation (17b,c) denote Lost-Work formulas derived from Equation (17a) for power-producing systems and power-consuming systems, respectively, where \dot{S}^{R_0} was substituted by Equation (18a) and Equation (18b) for power-producing systems and power-consuming systems, respectively.

$$\dot{W}^{LOST} = \dot{W}^{MAX} - \dot{W}^{Eq} \quad \{Power - Producing System\} \quad (16a)$$

$$\dot{W}^{LOST} = \dot{W}^{Eq} - (-\dot{W}^{MAX}) \quad \{Power - Consuming System\} \quad (16b)$$

$$\dot{W}^{LOST} = T_0 \dot{S}^{UNIV} = T_0 \left(\dot{S}^{R_0} + \sum_{i=1}^{Np} K_i \bar{S}_{K_i} - \sum_{i=1}^{Nf} G_i \bar{S}_{G_i} \right) \quad (17a)$$

$$\dot{W}^{LOST} = J^{LPS} \Delta \bar{H}_{LPS}^{VAP} \left(\frac{T_0}{T_{LPS}} \right) + J^{CW} \bar{C}_p^{CW} T_0 \cdot \ln \left(\frac{T_H^{CW}}{T_C^{CW}} \right) + T_0 \left(\sum_{i=1}^{Np} K_i \bar{S}_{K_i} - \sum_{i=1}^{Nf} G_i \bar{S}_{G_i} \right) \quad (17b)$$

$$\dot{W}^{LOST} = -J^{LPS} \Delta \bar{H}_{LPS}^{VAP} \left(\frac{T_0}{T_{LPS}} \right) + J^{CW} \bar{C}_p^{CW} T_0 \cdot \ln \left(\frac{T_H^{CW}}{T_C^{CW}} \right) + T_0 \left(\sum_{i=1}^{Np} K_i \bar{S}_{K_i} - \sum_{i=1}^{Nf} G_i \bar{S}_{G_i} \right) \quad (17c)$$

$$\dot{S}^{R_0} = \frac{\dot{Q}_{CW}^{R_0}}{T_0} + \frac{\dot{Q}_{LPS}^{R_0}}{T_0} = J^{CW} \bar{C}_p^{CW} \ln \left(\frac{T_H^{CW}}{T_C^{CW}} \right) + J^{LPS} \frac{\Delta \bar{H}_{LPS}^{VAP}}{T_{LPS}} \quad (18a)$$

$$\dot{S}^{R_0} = \frac{\dot{Q}_{CW}^{R_0}}{T_0} - \frac{\dot{Q}_{LPS}^{R_0}}{T_0} = J^{CW} \bar{C}_p^{CW} \ln \left(\frac{T_H^{CW}}{T_C^{CW}} \right) - J^{LPS} \frac{\Delta \bar{H}_{LPS}^{VAP}}{T_{LPS}} \quad (18b)$$

3. Results and Discussion

Technical and thermodynamic analyses of offshore GTW-EGR-CSS-CO₂-DEHY are presented and discussed.

3.1. Technical Assessment

Table 2 compiles the technical performance of offshore GTW-EGR-CCS-CO₂-DEHY. The NGCC plant, comprising five parallel NGCC elements, produces 599.3 MW of gross power ($\approx 92.4\%$ from gas turbines) entailing 534.4 MW of net exported power. Each gas

turbine generates ≈ 30 MW at 36.5% LHV-efficiency, firing ≈ 4.76 kg/s of gas. Due to the EGR, each NGCC element produces 370.6 kg/s of flue gas at 17.3%mol CO₂. The HRSG reduces the gas turbine flue gas temperature from 549 °C to 140 °C, which is the minimum value to maximize HPS output, providing enough LPS for PCC-MEA and CO₂-DEHY strippers.

Table 2. Technical analysis results.

GTW-EGR-CCS-CO ₂ -DEHY		Utilities Demand	Power (MW)	LPS (t/h)	CW (t/h)
CO ₂ flue gas (t/h) (PCC-MEA Feed)	557.2	NGCC plant	0.15	-	6109
CO ₂ emissions (t/h) (atmosphere)	59.6	PCC-MEA	0.35	1230	36,249
Gross power (MW)	599.3	CO ₂ -DEHY	0.00355	1.1	22.4
Power demand (MW)	64.9	CO ₂ -CMP-1	50.9	-	3894
Net power (MW)	534.4	CO ₂ -CMP-2	13.17	-	2324
		DCC	0.36	-	-
		STR-CO ₂	-	-	-
		Total	64.9	1231	48,598
PCC-MEA Results		CO ₂ -DEHY Results			
Flue gas inlet (%molCO ₂)	17.3	CO ₂ inlet (ppm-mol H ₂ O)	2690.2		
Decarbonated flue gas (%molCO ₂)	1.8	CO ₂ outlet (ppm-mol H ₂ O)	192.8		
CO ₂ to CO ₂ -CMP-1 (%molCO ₂)	92.7	Capture Ratio (kg ^{TEG} /kg ^{H₂O})	3.7		
Capture Ratio (kg ^{Solvent} /kg ^{CO₂})	13.7	Lean solvent (t/h)	2.1		
CO ₂ Captured (tCO ₂ /h)	497.6	Absorber: T ^{Top} (°C)/T ^{Bottom} (°C)	36.4/35.3		
Lean solvent (t/h)	6814	Stripper: T ^{Feed} (°C)/T ^{Top} (°C)/T ^{Bottom} (°C)	62/40/138		
Absorber: T ^{Top} (°C)/T ^{Bottom} (°C)	62.2/61.9	Reboiler duty (MW)	0.6		
Stripper: T ^{Feed} (°C)/T ^{Top} (°C)/T ^{Bottom} (°C)	83/40/103				
Heat Ratio (kJ/mol ^{CO₂})	225				
Reboiler duty (MW)	722				

The PCC-MEA stripper demands 722.2 MW of LPS and releases 144.2 kg/s of water-saturated CO₂ top product. CO₂-CMP-1 increases the pressure of the CO₂ stream up to 50 bar in order to achieve CO₂-DEHY ideal conditions. CO₂-DEHY captures $\approx 93\%$ of water from its feed and generates 503.8 t/h of Dry-CO₂ (≈ 193 ppm-mol H₂O). STR-CO₂ dispatches 5.3 t/h of low-pressure Dry-CO₂ to the TEG stripper reboiler as stripping gas to maintain its temperature below 140 °C, avoiding TEG degradation. The TEG stripper reboiler requires only 0.6 MW of LPS, since the flowrate of captured water from the CO₂ stream is small. CO₂-CMP-2 sends 498.8 t/h of Dry-CO₂ (P = 300 bar, T = 35 °C) to EOR. The Offshore GTW-EGR-CCS-CO₂-DEHY power requirement corresponds to 10.8% of its gross power. CO₂-CMP-1 and CO₂-CMP-2 units are the major electricity consumers, while PCC-MEA leads LPS and CW consumptions.

3.2. Thermodynamic Analysis

Thermodynamic and Lost-Work analyses were accomplished for the offshore GTW-EGR-CCS-CO₂-DEHY overall system and its sub-systems, namely (i) NGCC plant; (ii) DCC; (iii) PCC-MEA; (iv) CO₂-CMP-1; (v) CO₂-DEHY; (vi) STR-CO₂; and (vii) CO₂-CMP-2. No sub-system was missed, i.e., the GTW-EGR-CCS-CO₂-DEHY is correctly partitioned among the sub-systems mentioned, which means that the respective sums of \dot{W}^{MAX} , \dot{W}^{Eq} , and \dot{W}^{LOST} for all sub-systems must deliver the same value of the overall system, which is calculated independently of the sub-systems. The comparison of the overall system values with the respective sum over the sub-systems entails an indirect consistency check of the thermodynamic analysis. It is worth mentioning that there is always some divergence between the overall system and the sums over the sub-systems in practice. Thus, divergences below 1% can be accepted to validate the consistency of the thermodynamic analysis.

3.2.1. Maximum Power, Equivalent Power, and Thermodynamic Efficiency Results

Table 3 shows the thermodynamic efficiencies and other second law analysis results of the offshore GTW-EGR-CCS-CO₂-DEHY and its sub-systems. The overall system, NGCC plant, DCC, and STR-CO₂, are power-producing systems ($\dot{W}^{MAX} > 0$); thus, Equations (13a)–(16a), (17b), and (18a) were used for \dot{W}^{Eq} , $\eta\%$, \dot{W}^{LOST} . Furthermore, sub-systems PCC-MEA, CO₂-CMP-1, CO₂-DEHY, and CO₂-CMP-2 are power-consuming systems ($\dot{W}^{MAX} < 0$), requiring Equations (13b)–(16b), (17c), and (18b) for \dot{W}^{Eq} , $\eta\%$, \dot{W}^{LOST} . The overall offshore GTW-EGR-CCS-CO₂-DEHY thermodynamic efficiency reaches 33.35% (Table 3).

Table 3. Second law analysis and Lost-Work validation.

Sub-System	Second Law Analysis						Lost-Work Validation		
	\dot{W}^{MAX} (MW)	\dot{W}_{LPS}^{Eq} (MW)	\dot{W}_{CW}^{Eq} (MW)	$\dot{E}E$ (MW)	\dot{W}^{Eq} (MW)	$\eta\%$	\dot{W}^{LOST} (MW) *	\dot{W}^{LOST} (MW) #	$\Delta\dot{W}^{LOST}$ (%)
NGCC plant	1678.12	212.37	4.40	599.18	815.96	48.62%	862.16	860.66	0.17
PCC-MEA	−31.29	212.19	31.41	0.35	181.14	17.27%	149.85	149.03	0.55
CO ₂ -DEHY	−0.00014	0.18	0.07	0.00355	0.12	0.12%	0.1193	0.1189	0.34
CO ₂ -CMP-1	−28.41	-	2.81	50.90	48.09	59.09%	19.67	19.74	−0.36
CO ₂ -CMP-2	−4.88	-	1.68	13.17	11.49	42.49%	6.61	6.59	0.30
DCC	26.31	-	-	−0.36	−0.36	−1.37%	26.67	26.50	0.64
STR-CO ₂	0.48	-	-	-	-	0.00%	0.480	0.478	0.42
Sum-crosscheck							1065.56	1063.12	0.23
Overall system	1602.33	-	-	534.40	534.40	33.35%	1067.93	1061.74	0.58

* via Equation (16a,b); # via Equation (17b,c).

Totalling a positive $\dot{W}^{MAX} = 1678.12$ MW, the NGCC plant is clearly a power-producing system as a result of its highly spontaneous transitions (e.g., combustion) inside the NGCC elements. The \dot{W}^{Eq} generated by each NGCC element is calculated as follows: $\dot{E}E$ is produced as gas turbines power plus steam turbine power minus the Rankine cycle pump power (Figure 2), it is added to \dot{W}_{CW}^{Eq} generated by the Rankine cycle condenser, and then it is added to \dot{W}_{LPS}^{Eq} from the HRSG LPS exportation. The thermodynamic efficiency of the NGCC plant reached 48.62%.

CW is a process stream suffering evaporation loss in the flue gas–liquid direct contact of DCC, so CW should not be considered a utility ($\dot{W}_{CW}^{Eq} = 0$) in the DCC. In addition, LPS was not consumed ($\dot{W}_{LPS}^{Eq} = 0$). Therefore, only $\dot{E}E$ from the pump contributes (negatively) to \dot{W}^{Eq} . DCC \dot{W}^{Eq} is negative because it is a power-producing system performing spontaneous changes ($\dot{W}^{MAX} > 0$), but electricity is consumed instead of produced.

As with any separation process, PCC-MEA is a power-consuming system. As expected, PCC-MEA \dot{W}^{MAX} is negative (−31.29 MW) due to the equivalent power required for CO₂ separation from flue gas. PCC-MEA \dot{W}^{Eq} consumption (181.14 MW) is measured as follows: electricity demanded in a solvent recirculation pump and water make-up pump is added to \dot{W}_{LPS}^{Eq} consumed in the PCC-MEA stripper reboiler, and \dot{W}_{CW}^{Eq} exported as hot-CW from the PCC-MEA stripper condenser and from the lean-MEA cooler are subtracted. The PCC-MEA thermodynamic efficiency reaches 17.27%.

Another separation process, CO₂-DEHY, is also a power-consuming system ($\dot{W}^{MAX} = -0.00014$ MW). The \dot{W}^{MAX} incredibly small value is due to the almost counter-balance of three small opposed factors: (i) the small water flowrate removed from CO₂ stream (≈ 2700 ppm-mol H₂O to ≈ 200 ppm-mol H₂O), which evidently is a separation

that demands small power consumption ($\dot{W}^{MAX} < 0$); (ii) the positive power which could be produced by expanding streams through the head losses generated in the absorber, stripping column, and heat exchangers ($\dot{W}^{MAX} > 0$); and (iii) the positive power which could be produced by the utilization of the thermal approaches in heat exchangers, the stripper reboiler, and stripper condenser. As a result, CO₂-DEHY has a minimum net power demand to perform water removal from the CO₂ of only 0.00014 MW. On the other hand, CO₂-DEHY has \dot{W}^{Eq} (0.12 MW) calculated as follows: (i) $\dot{E}E$ consumed in TEG recirculation pumps, added to \dot{W}_{LPS}^{Eq} consumed through LPS consumption in the stripper reboiler, subtracted from \dot{W}_{CW}^{Eq} exported through hot-CW from the stripper condenser and from the lean-TEG cooler. The CO₂-DEHY thermodynamic efficiency reaches 0.12% (0.00014 MW*100/0.12 MW).

STR-CO₂ is another sub-system guided by spontaneities; in other words, it is a power-producing system ($\dot{W}^{MAX} = 0.48$ MW), but its thermodynamic efficiency is 0%. The underlying reason is because $\dot{E}E$, \dot{W}_{LPS}^{Eq} , and \dot{W}_{CW}^{Eq} are all zero. This means that STR-CO₂ has sufficient spontaneities to produce power, but this potential is wasted, and zero power is produced. Consequently, the STR-CO₂ thermodynamic efficiency is zero.

CO₂-CMP-1 and CO₂-CMP-2 are obvious power-consuming systems ($\dot{W}^{MAX} = -28.41$ MW and $\dot{W}^{MAX} = -4.88$ MW, respectively) because they perform non-spontaneous compression. The respective \dot{W}^{Eq} is obtained as follows: $\dot{E}E$ consumed in compressors and pump, minus \dot{W}_{CW}^{Eq} exported as hot-CW from compressor intercoolers (there is no LPS consumption, i.e., $\dot{W}_{LPS}^{Eq} = 0$). The CO₂-CMP-1 and CO₂-CMP-2 thermodynamic efficiencies are 59.09% and 42.49%, respectively.

3.2.2. Lost-Work Analysis

Lost-Work exposes the power potential destroyed in GTW-EGR-CCS-CO₂-DEHY and in its sub-systems due to spontaneities. Table 3 reveals the Lost-Work results and also attests the consistency of the present thermodynamic analysis by comparing Lost-Work values calculated through two thermodynamically independent ways: (i) via \dot{W}^{MAX} and \dot{W}^{Eq} in Equation (16a,b) and (ii) via $T_0 \cdot \dot{S}^{UNIV}$ in Equation (17b,c) for power-producing and power-consuming systems, respectively. In addition, Table 3 proves a consistency crosscheck in the sum of Lost-Works over sub-systems which, theoretically, should be equal to the overall-system Lost-Work (obtained divergences are smaller than 1%).

Figure 8 illustrates Sankey diagrams for \dot{W}^{MAX} , \dot{W}^{Eq} , and \dot{W}^{LOST} flows for the overall system and its sub-systems, in which \dot{W}^{LOST} represents the sum of Lost-Works over sub-systems (light-red flows), while $\Delta \dot{W}^{LOST}$ is its difference from the overall system Lost-Work (Table 3). In total, 66.65% of the offshore GTW-EGR-CCS-CO₂-DEHY available power ($\dot{W}^{MAX} = 1602.33$ MW) is wasted as Lost-Work through process spontaneities, which are mainly (i) combustion spontaneity and mixing in gas turbines; (ii) heat transfer finite thermal approaches; (iii) finite head losses; (iv) mixing of streams in several units; and (v) machine irreversibility, with compressor/expander adiabatic efficiencies lower than 100%.

The NGCC plant has the highest \dot{W}^{LOST} (832.2 MW, 80.7% share) by virtue of extremely spontaneous combustion reactions, followed by PCC-MEA (149.9 MW, 14.0% share) as consequence of its mass transfer finite potentials in columns, stream mixing, thermal approaches in exchangers, and columns/exchangers head losses. The Lost-Works of the other sub-systems are still smaller because these sub-systems are rather small in importance: DCC (26.7 MW, 2.5% share), CO₂-CMP-1 (19.7 MW, 1.8% share), CO₂-CMP-2 (6.6 MW, 0.6% share), STR-CO₂ (0.48 MW, 0.04% share), and CO₂-DEHY (0.1 MW, 0.01% share).

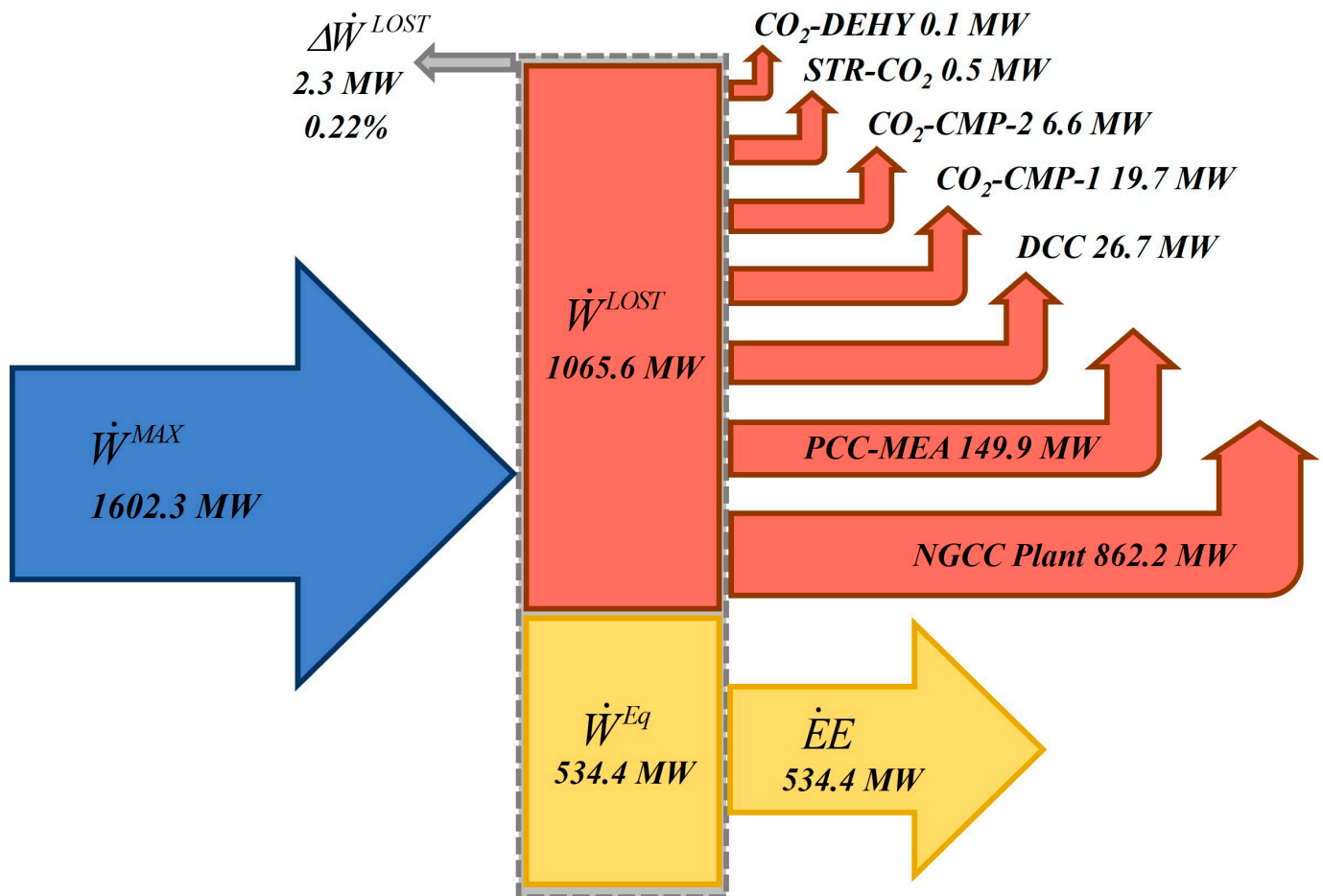


Figure 8. Lost-Work Sankey diagram (\dot{E} : electricity, \dot{W}^{MAX} : maximum power, \dot{W}^{LOST} : Lost-Work, \dot{W}^{Eq} : equivalent power, NGCC: NG Combined Cycle, DCC: Direct-Contact Column, PCC-MEA: Aqueous-MEA Post-Combustion Capture, CO₂-CMP: CO₂ Compression Unit, CO₂-DEHY: CO₂ Dehydration TEG Unit, SGU-CO₂: CO₂ Stripping Gas Unit).

4. Conclusions

Technical and thermodynamic analyses of a theoretically environmentally friendly (low-emission) and new offshore GTW-EGR-CCS-CO₂-DEHY process were conducted. The offshore GTW-EGR-CCS-CO₂-DEHY burns ≈ 6.5 MMSm³/d of CO₂-rich NG (CO₂ > 40%mol), exports low-emission electricity, and sends dense CO₂ to EOR. The offshore GTW-EGR-CCS-CO₂-DEHY produces 534.4 MW of net power, abating $\approx 90\%$ of flue gas CO₂. The offshore GTW-EGR-CCS-CO₂-DEHY is an intensified power production process, whose major intensification components comprehend the following: (i) Exhaust Gas Recycle (EGR), which reduces the flue gas flowrate by $\approx 65\%$ while increasing its CO₂ content from $\approx 7\%$ mol up to $\approx 17\%$ mol, and (ii) high-pressure CO₂ dehydration in CO₂-DEHY, which extracts $\approx 93\%$ of water from the CO₂-to-EOR stream (≈ 200 ppm-mol H₂O), avoiding the formation of hydrates in EOR pipelines. The advantage brought about by EGR is that it dismisses air excess (typically $\approx 100\%$) for gas turbine flame temperature reduction, consequently decreasing $\approx 65\%$ the flue gas volumetric flowrate and raising its CO₂ content from typical $\approx 7\%$ mol (without EGR) to $\approx 17\%$ mol (with EGR). Thus, EGR drastically lowers investment and the operational cost of the CCS plant by reducing column diameter/height and improving low-emission GTW profitability.

The second law analysis of the offshore GTW-EGR-CCS-CO₂-DEHY overall system reveals a 33.35% thermodynamic efficiency with 66.65% of Lost-Work, making the NGCC sub-system the greatest Lost-Work sink (80.7% \dot{W}^{LOST} share) due to the highly spontaneous

gas turbine firing process. The PCC-MEA sub-system is the second largest Lost-Work sink (14.0% W^{LOST} share). Therefore, the NGCC and PCC-MEA are the major GTW-EGR-CCS-CO₂-DEHY units that need to be upgraded to improve the efficiency of the overall system to attain better economic and environmental benefits. The consistency of the thermodynamic analysis was settled via Lost-Work sum-crosschecks and lateral checks considering the alternative second law formula $T_0 \cdot \dot{S}^{UNIV}$ for the Lost-Work (Table 3).

The technological innovations associated with the new proposed offshore GTW-EGR-CCS-CO₂-DEHY process are not related to the units that constitute it because all these units and the adopted intensification strategies (such as EGR and CO₂ dehydration) are well known and individually techno-economically feasible. Instead, one could say that the most important innovation is the overall process configuration and the new possible interactions that emerge among the units that constitute the new process. These interactions obviously occur in the steady-state context as well as in the dynamic and controllability contexts, and they are very different depending on the context. It was demonstrated in the steady-state context, for example, that in spite of the gigantism of the new process and its main complex objective of generating low-emission electricity by firing CO₂-rich NG at remote offshore sites, its thermodynamic efficiency is still reasonable, and its revenues are improved by exporting tradable CO₂ as an EOR agent, which boosts oil production while being confined in the reservoir.

In other words, the main contribution associated with this study is that it proves that the new process accomplishes its finalities and is thermodynamically, environmentally, and economically feasible. That is, it configures an expensive technological package that is worthwhile of further study, aiming at achieving large-scale implementation.

5. Suggestions for Future Work

The comparison of the efficiency and other performance (economic, environmental, thermodynamic) aspects of the newly proposed process against conventional counterparts is a very relevant point. It is also relevant to compare our proposed thermodynamic analysis of processes against alternative analyses such as the exergy analysis of processes, which is much more present in the literature. But these recommendations are also somewhat out of the present scope, which is already overburdened. Thus, we recommend that future works are dedicated to these important comparisons. The authors suggest carrying out an exergy analysis of the GTW-EGR-CCS-CO₂-DEHY process and a subsequent comparison of it against conventional counterparts. Although the exergy analysis of processes is formally different from the thermodynamic analysis of processes, they normally point in the same direction, since both aim at revealing the weak (less thermodynamically efficient) units in the process that mostly require improvement. In addition to the exergy analysis, the efficiency and performance aspects (economic, environmental, and thermodynamic) of the GTW-EGR-CCS-CO₂-DEHY process should be compared against existing offshore NGCC concepts.

Author Contributions: Conceptualization J.L.d.M.; methodology J.L.d.M. and O.d.Q.F.A.; formal analysis, A.d.C.R., J.L.d.M. and O.d.Q.F.A.; investigation, A.d.C.R. and J.L.d.M.; data curation, A.d.C.R.; writing—original draft preparation, A.d.C.R. and J.L.d.M.; visualization, A.d.C.R. and J.L.d.M.; writing—review and editing, J.L.d.M. and O.d.Q.F.A.; supervision, J.L.d.M. and O.d.Q.F.A.; project administration, J.L.d.M. and O.d.Q.F.A. All authors have read and agreed to the published version of the manuscript.

Funding: Authors acknowledge financial support from Petrobras S/A (5850.0107386.18.9). JL de Medeiros and OQF Araújo also acknowledge support from CNPq-Brazil (313861/2020-0, 312328/2021-4) and from FAPERJ Brazil (E-26/200.522/2023, E-26/201.178/2021). AC Reis acknowledges financial support from FAPERJ Brazil (E-26/203.508/2023).

Data Availability Statement: Data are contained within the article.

Conflicts of Interest: The authors declare no potential conflicts of interest with respect to the research, authorship, and/or publication of this article.

Nomenclature

\dot{E}	Electricity (MW)
G_i	Flowrate of i th feed stream (kmol/s)
\bar{H}	Molar enthalpy (MJ/kmol)
K_i	Flowrate of i th product stream (kmol/s)
N_f	Number of feed streams (inputs)
N_p	Number of product streams (outputs)
P	Pressure (bar)
\dot{Q}, \bar{S}	Heat duty (MW), molar entropy (MJ/K·kmol)
T, W	Temperature (K), power (MW)
η	Thermodynamic efficiency (%)
CW, Eq, LPS	Cooling Water, equivalent, Low-Pressure Steam

References

- Neseli, M.A.; Ozgener, O.; Ozgener, L. Energy and exergy analysis of electricity generation from natural gas pressure reducing stations. *Energy Convers. Manag.* **2015**, *93*, 109–120. [[CrossRef](#)]
- de Freitas, V.A.; Vital, J.C.S.; Rodrigues, B.R.; Rodrigues, R. Source rock potential, main depocenters, and CO₂ occurrence in the pre-salt section of Santos Basin, southeast Brazil. *J. S. Am. Earth Sci.* **2022**, *115*, 103760. [[CrossRef](#)]
- Andrei, M.; Sammarco, G. Gas to wire with carbon capture & storage: A sustainable way for on-site power generation by produced gas. In Proceedings of the Abu Dhabi International Petroleum Exhibition and Conference, Abu Dhabi, United Arab Emirates, 13–16 January 2017. [[CrossRef](#)]
- Ojjiagwo, E.; Oduoza, C.F.; Emekwuru, N. Economics of gas to wire technology applied in gas flare management. *Eng. Sci. Technol. Int. J.* **2016**, *19*, 2109–2118. [[CrossRef](#)]
- Sayed, S.; Massoud, A. Minimum transmission power loss in multi-terminal HVDC systems: A general methodology for radial and mesh networks. *Alex. Eng. J.* **2019**, *58*, 115–125. [[CrossRef](#)]
- Watanabe, T.; Inoue, H.; Horitsugi, M.; Oya, S. Gas to Wire (GTW) system for developing ‘small gas field’ and exploiting ‘associated gas’. In Proceedings of the SPE International Oil and Gas Conference and Exhibition in China, Beijing, China, 5–7 December 2006; Volume 1, pp. 310–315.
- Brito, T.L.F.; Galvão, C.; Fonseca, A.F.; Costa, H.K.M.; Moutinho dos Santos, E. A review of gas-to-wire (GtW) projects worldwide: State-of-art and developments. *Energy Policy* **2022**, *163*, 112859. [[CrossRef](#)]
- Zhou, D.; Li, P.; Liang, X.; Liu, M.; Wang, L. A long-term strategic plan of offshore CO₂ transport and storage in northern South China Sea for a low-carbon development in Guangdong province, China. *Int. J. Greenh. Gas. Control* **2018**, *70*, 76–87. [[CrossRef](#)]
- Roussanaly, S.; Aasen, A.; Anantharaman, R.; Danielsen, B.; Jakobsen, J.; Heme-De-Lacotte, L.; Neji, G.; Sødal, A.; Wahl, P.; Vrana, T.; et al. Offshore power generation with carbon capture and storage to decarbonise mainland electricity and offshore oil and gas installations: A techno-economic analysis. *Appl. Energy* **2019**, *233–234*, 478–494. [[CrossRef](#)]
- Zhao, H.; Chang, Y.; Feng, S. Influence of produced natural gas on CO₂-crude oil systems and the cyclic CO₂ injection process. *J. Nat. Gas. Sci. Eng.* **2016**, *35*, 144–151. [[CrossRef](#)]
- Monson, C.C.; Korose, C.P.; Frailey, S.M. Screening methodology for regional-scale CO₂ EOR and storage using economic criteria. *Energy Procedia* **2014**, *63*, 7796–7808. [[CrossRef](#)]
- Hassanpouryouzband, A.; Yang, J.; Tohidi, B.; Chuvilin, E.; Istomin, V.; Bukhanov, B. Geological CO₂ Capture and Storage with Flue Gas Hydrate Formation in Frozen and Unfrozen Sediments: Method Development, Real Time-Scale Kinetic Characteristics, Efficiency, and Clathrate Structural Transition. *ACS Sustain. Chem. Eng.* **2019**, *7*, 5338–5345. [[CrossRef](#)]
- Hassanpouryouzband, A.; Yang, J.; Tohidi, B.; Chuvilin, E.; Istomin, V.; Bukhanov, B.; Cheremisin, A. CO₂ Capture by Injection of Flue Gas or CO₂-N₂ Mixtures into Hydrate Reservoirs: Dependence of CO₂ Capture Efficiency on Gas Hydrate Reservoir Conditions. *Environ. Sci. Technol.* **2018**, *52*, 4324–4330. [[CrossRef](#)]
- Wu, M.; Jiang, C.; Song, R.; Liu, J.; Li, M.; Liu, B.; Shi, D.; Zhu, Z.; Deng, B. Comparative study on hydraulic fracturing using different discrete fracture network modeling: Insight from homogeneous to heterogeneity reservoirs. *Eng. Fract. Mech.* **2023**, *284*, 109274. [[CrossRef](#)]
- Huang, L.; Dontsov, E.; Fu, H.; Lei, Y.; Weng, D.; Zhang, F. Hydraulic fracture height growth in layered rocks: Perspective from DEM simulation of different propagation regimes. *Int. J. Solids Struct.* **2022**, *238*, 111395. [[CrossRef](#)]
- Araújo, O.Q.F.; Reis, A.d.C.; de Medeiros, J.L.; Nascimento, J.F.D.; Grava, W.M.; Musse, A.P.S. Comparative analysis of separation technologies for processing carbon dioxide rich natural gas in ultra-deepwater oil fields. *J. Clean. Prod.* **2017**, *155*, 12–22. [[CrossRef](#)]

17. Hetland, J.; Kvamsdal, H.M.; Haugen, G.; Major, F.; Kårstad, V.; Tjellander, G. Integrating a full carbon capture scheme onto a 450 MWe NGCC electric power generation hub for offshore operations: Presenting the Sevan GTW concept. *Appl. Energy* **2009**, *86*, 2298–2307. [[CrossRef](#)]
18. Hachem, J.; Schuhler, T.; Orhon, D.; Cuif-Sjostrand, M.; Zoughaib, A.; Molière, M. Exhaust gas recirculation applied to single-shaft gas turbines: An energy and exergy approach. *Energy* **2022**, *238*, 121656. [[CrossRef](#)]
19. Li, H.; Ditaranto, M.; Yan, J. Carbon capture with low energy penalty: Supplementary fired natural gas combined cycles. *Appl. Energy* **2012**, *97*, 164–169. [[CrossRef](#)]
20. Li, H.; Ditaranto, M.; Berstad, D. Technologies for increasing CO₂ concentration in exhaust gas from natural gas-fired power production with post-combustion, amine-based CO₂ capture. *Energy* **2011**, *36*, 1124–1133. [[CrossRef](#)]
21. Ahmadi, M.A.; Soleimani, R.; Bahadori, A. A computational intelligence scheme for prediction equilibrium water dew point of natural gas in TEG dehydration systems. *Fuel* **2014**, *137*, 145–154. [[CrossRef](#)]
22. Kloster, P. Energy Optimization on Offshore Installations with Emphasis on Offshore Combined Cycle Plants. In Proceedings of the SPE Offshore Europe Conference and Exhibition, Aberdeen, UK, 7–10 September 1999; Society of Petroleum Engineers: Aberdeen, UK, 1999. *Epub ahead of print*. [[CrossRef](#)]
23. GE LM2500+G4 Marine Gas Turbine. 2021. Available online: <https://www.geaviation.com/sites/default/files/datasheet-lm2500plusg4.pdf> (accessed on 2 August 2022).
24. Følgesvold, E.R.; Skjefstad, H.S.; Riboldi, L.; Nord, L.O. Combined heat and power plant on offshore oil and gas installations. *J. Power Technol.* **2017**, *97*, 117–126.
25. Oh, S.-Y.; Binns, M.; Cho, H.; Kim, J.-K. Energy minimization of MEA-based CO₂ capture process. *Appl. Energy* **2016**, *169*, 353–362. [[CrossRef](#)]
26. Araújo, O.Q.F.; de Medeiros, J.L. Carbon capture and storage technologies: Present scenario and drivers of innovation. *Curr. Opin. Chem. Eng.* **2017**, *17*, 22–34. [[CrossRef](#)]
27. Liu, G.; Zhu, L.; Hong, J.; Liu, H. Technical, Economical, and Environmental Performance Assessment of an Improved Triethylene Glycol Dehydration Process for Shale Gas. *ACS Omega* **2022**, *7*, 1861–1873. [[CrossRef](#)] [[PubMed](#)]
28. Neagu, M.; Cursaru, D.L. Technical and economic evaluations of the triethylene glycol regeneration processes in natural gas dehydration plants. *J. Nat. Gas. Sci. Eng.* **2017**, *37*, 327–340. [[CrossRef](#)]
29. Chebbi, R.; Qasim, M.; Abdel Jabbar, N. Optimization of triethylene glycol dehydration of natural gas. *Energy Rep.* **2019**, *5*, 723–732. [[CrossRef](#)]
30. Mokhatab, S.; Poe, W.A.; Mak, J.Y. Natural Gas Dehydration and Mercaptans Removal. *Handb. Nat. Gas. Transm. Process* **2019**, *4*, 307–348. [[CrossRef](#)]
31. Milão, R.d.F.D.; de Medeiros, J.L.; Interlenghi, S.F.; Araújo, O.d.Q.F. Low-emission Gas-to-Wire with thermodynamic efficiency: Monetization of carbon dioxide rich natural gas from offshore fields. *Gas Sci. Eng.* **2023**, *115*, 205021. [[CrossRef](#)]

Disclaimer/Publisher’s Note: The statements, opinions and data contained in all publications are solely those of the individual author(s) and contributor(s) and not of MDPI and/or the editor(s). MDPI and/or the editor(s) disclaim responsibility for any injury to people or property resulting from any ideas, methods, instructions or products referred to in the content.